Proc. NIPR Symp. Antarct. Meteorites, **9**, 111–126, 1996

THE KINETICS AND MECHANISM OF IRON SULFIDE FORMATION IN THE SOLAR NEBULA

Dante S. LAURETTA[1,2], Bruce FEGLEY, Jr.[1,2], Katharina LODDERS[1,2] and Daniel T. KREMSER[2]

[1]*Planetary Chemistry Laboratory,*
[2]*Department of Earth and Planetary Sciences,*
Campus Box 1169, Washington University, One Brookings Drive, St. Louis, MO 63130-4899, U.S.A.

Abstract: We summarize an experimental study of the kinetics and mechanism of FeS formation by the reaction of H_2S-H_2 gas mixtures with iron metal. Characterization of the reacted samples by optical microscopy, X-ray diffraction, electron microprobe analyses, and gravimetric analyses provided detailed information on the Fe/S ratio, microstructure and morphology, and formation kinetics of the iron sulfide layers. The Fe/S ratios of the iron sulfide layers varied from $Fe_{0.90}S$ to FeS with temperature and gas composition, in agreement with models of gas-solid equilibrium. The morphology, microstructure, and growth orientation of the sulfide layers also varied with temperature and gas composition. Typically, sulfide layer growth proceeded by the development of a compact, uniformly oriented scale which later cracked when it could no longer plastically deform. Further reaction led to the growth of a finer grained, randomly oriented, highly porous inner layer between the metal and original sulfide scale. Initially sulfide layers grew linearly with time with the kinetics controlled by chemical reactions at the gas-solid interface. However, upon reaching a critical thickness, diffusion through the sulfide scale became the rate limiting step and layer growth followed parabolic kinetics. The linear and parabolic rate constants for iron sulfide growth were determined and then used to constrain FeS formation in the solar nebula. FeS formation is rapid compared to estimated nebular lifetimes of 1–10 million years. Our results also imply that the variations in the sulfur content of chondritic material are due to removal of metal grains from contact with the gas (*e.g.*, by accretion into larger bodies) at temperatures above 400 K, where complete sulfur condensation occurs, rather than by kinetic inhibition of gas-solid equilibrium between H_2S gas and iron metal grains.

1. Introduction

Nearly 50 years ago, Harold UREY began studying the origin and evolution of the solar system and investigated the importance of chemical reactions between gas and dust in the solar nebula for determining the compositions of the solid grains which eventually grew in size and were accreted to form the planets, asteroids, comets, and meteorites in our solar system (UREY, 1952). Being a physical chemist, UREY applied chemical thermodynamics to predict the course of chemical reactions as the solar nebula cooled down. However, he realized that this approach, although quite powerful, was only the first step needed to unravel the true course of events and he discussed thermodynamic modeling of chemical reactions in the solar nebula as follows (UREY, 1953): "Our data in

this field give much information relative to possible reactions, and at higher temperatures they certainly give us practically assured knowledge of the chemical situations due to the high velocities of reactions, at least in homogeneous systems, providing the data are adequate, which is unfortunately not always the case. At lower temperatures thermodynamic equilibrium may not be reached even in periods of time that are long compared to the age of the universe, and at these temperatures the kinetics of thermal reactions or of photochemical reactions become important."

Despite the powerful influence that UREY's work had in shaping the new field of cosmochemistry, his early recognition of the importance of chemical kinetics for modeling nebular chemistry was generally ignored until the 1980s when theoretical work began to be done on the kinetics of gas phase reactions in the solar nebula (*e.g.*, LEWIS and PRINN, 1980; PRINN and FEGLEY, 1981, 1989; FEGLEY and PRINN, 1989). This work showed that kinetics, and not equilibrium thermodynamics controlled the speciation of carbon and nitrogen in the solar nebula gas. For example, CO and N_2 are predicted to be the dominant carbon and nitrogen gases throughout the entire solar nebula, while CH_4 and NH_3 comprise only very minor amounts of the total carbon and nitrogen in the solar nebula.

The important role played by kinetics for gas phase chemistry in the solar nebula naturally suggested that kinetics may also play an important role in gas-grain chemistry in the solar nebula. Several papers in the late 1980s and early 1990s (*e.g.*, PRINN and FEGLEY, 1987, 1989; FEGLEY, 1988, 1993; FEGLEY and PRINN, 1989) described theoretical models of gas-grain kinetics using a simple collision theory (SCT) first presented by FEGLEY (1988). This work predicted the rates of gas-grain reactions that form three important minerals found in meteorites: hydrated silicates, magnetite, and troilite. The SCT calculations assumed that grains were monodispersed spheres comparable in size to interstellar dust and fine-grained meteorite matrix (~0.1 μm radius), and used the kinetic theory of gases and kinetic data from the materials science literature to estimate the reactive fraction of collisions, and to calculate the chemical lifetime (t_{chem}=–[i]/d[i]/dt where [i] is the number density of species i) of the different reactions. Unless the t_{chem} value for a reaction is less than or equal to the nebular lifetime, the reaction is too slow to take place during the nebular lifetime of 1–10 million years (PODOSEK and CASSEN, 1994). The SCT models predicted that the t_{chem} value for hydrated silicate formation is about 4.5 billion years, that the t_{chem} for magnetite formation is about 320000 years, and that the t_{chem} for troilite formation is only 320 years (FEGLEY, 1988).

Although the SCT models provide important insights into the rates of gas-grain reactions in the solar nebula, experimental studies of gas-grain reactions such as hydrated silicate formation, magnetite formation, or troilite formation are important to understand the kinetics and mechanisms of these reactions. Because no prior experimental studies have been done, we started a program to investigate gas-grain kinetics under temperature, composition (and eventually pressure) conditions relevant to the solar nebula. Preliminary results of these studies were reported earlier (LAURETTA and FEGLEY, 1994a, b, c; LAURETTA *et al.*, 1995a, b).

Here we present some results of our study of the kinetics and mechanism of troilite formation via the net thermochemical reaction:

$$Fe(metal) + H_2S(gas)=FeS(solid) + H_2(gas). \quad (1)$$

We decided to study this reaction first for several reasons. The SCT models predict that troilite formation is very rapid, and indeed we found that most experiments could be done in hours to weeks. Also, sulfur is the tenth most abundant element in solar material and is the second most abundant volatile element, after oxygen, in meteorites. Finally, troilite is ubiquitous in meteorites, so an understanding of how it formed in the solar nebula is important for interpreting the record of nebular chemistry preserved, with varying degrees of fidelity, in chondrites.

2. Experimental Procedures

High purity iron foils (Johnson-Matthey Puratronic grade 99.998% pure on a metals basis) that were ~1 cm^2 with nominal thicknesses of either 0.025 cm or 0.050 cm were used in the experiments. Prior to being reacted, the foils were carefully weighed and measured. The foils were then annealed in prepurified H_2 (>99.99%) for at least 20 hours at 750°C. The iron foils were cooled to the desired reaction temperature in the prepurified H_2, and were then isothermally heated in H_2S-H_2 gas mixtures at atmospheric pressure for varying time periods. The nominal H_2S contents of the gas mixtures were 25, 50, 100, 1000, and 10000 parts per million by volume (ppmv). For reference, the solar S/H elemental abundance ratio (ANDERS and GREVESSE, 1989; DREIBUS *et al.*, 1995) corresponds to ~33 ppmv H_2S in the solar nebula where troilite forms. After heating, the H_2S-H_2 gas flow was replaced by prepurified N_2, the samples were pulled into a cooled gas tight fitting outside the furnace, and cooled down.

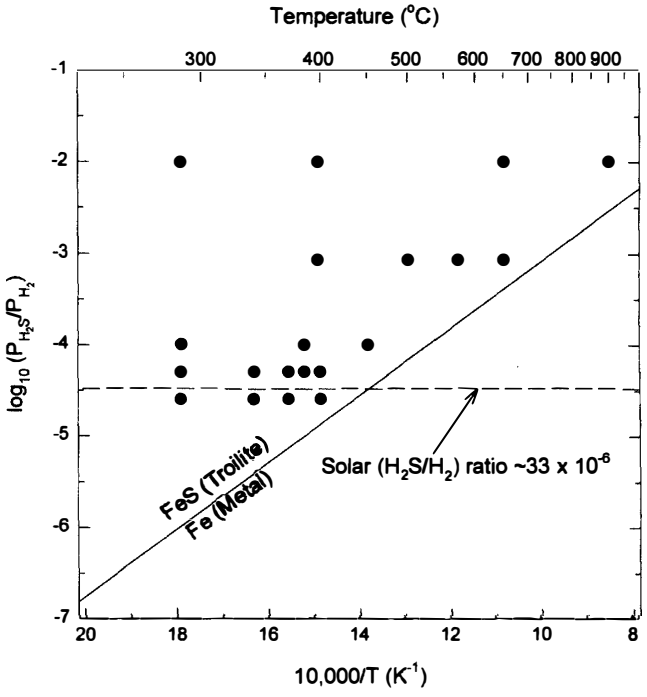

Fig. 1. The Fe/FeS phase boundary (diagonal line) and the locations of the iron sulfide formation experiments (black dots). The horizontal dashed line shows the expected H_2S/H_2 ratio in the solar nebula assuming solar composition (ANDERS and GREVESSE. 1989; DREIBUS et al., 1995). Chemical equilibrium calculations of nebular chemistry predict that H_2S is the major sulfur gas at these low temperatures. The Fe/FeS phase boundary was calculated using the latest thermodynamic data for $H_2S(g)$ and iron sulfides (CHASE et al., 1985; GRØNVOLD et al., 1991; GRØNVOLD and STØLEN, 1992). The intersection of the two lines, at 713 K, is the FeS formation temperature (from pure Fe metal) in the solar nebula.

About 120 experiments were done to determine the effects of temperature and H_2S/H_2 ratio, and to determine if reaction rates were proportional to time (linear kinetics) or proportional to time squared (parabolic kinetics). The black points on Fig. 1 show the temperatures and H_2S/H_2 ratios where the different series of experiments were done. Additional details of the experimental and analytical procedures are given in LAURETTA *et al.* (1996a, b).

3. Chemical Composition of Sulfide Layers

The sulfide layers on the reacted samples were chemically analyzed by X-ray diffraction (XRD), electron microprobe (EMP) analysis, and gravimetric analysis by quantitative combustion to hematite. In many cases, electron microprobe traverses across the sulfide layers were also done. Table 1 summarizes the analytical data for the bulk composition of the sulfide layers. There is good agreement between the results from the three methods. A comparison of the observed Fe/S ratios to those predicted from the defect thermodynamics model of LIBOWITZ (1972) shows that with a few exceptions (*e.g.*, low temperature runs in 50 ppmv H_2S gas mixtures), the observed Fe/S ratios are the same within the analytical uncertainties as those predicted from gas-solid equilibrium (LIBOWITZ, 1972; RAU, 1976). Also, cracking of sulfide layers in some 10000 ppmv runs exposed fresh metal to gas leading to disagreements between predicted and observed Fe/

Table 1. Observed and predicted compositions of iron sulfides from kinetic experiments.

Temp.	Fe/S atomic ratio					
(K)	XRD[a]	Microprobe[a]	Combustion[a]	Mean	Predicted	Δ(%)[b]
			50 ppm H_2S			
558	0.956	0.962	n.a.	0.959	0.994	–3.6
613	0.957	0.949	n.a.	0.953	0.997	–4.6
673	0.988	0.982	n.a.	0.985	0.998	–1.3
			100 ppm H_2S			
558	0.972	0.988	n.a.	0.980	0.991	–1.1
658	0.997	0.996	n.a.	0.997	0.996	0.1
723	1.004	0.965	n.a.	0.985	0.998	–1.3
			850 ppm H_2S			
673	0.990	0.986	n.a.	0.988	0.987	0.1
778	0.996	0.988	0.985	0.990	0.993	–0.3
848	0.999	0.979	0.989	0.989	0.995	–0.6
923	0.990	0.989	0.992	0.990	0.997	–0.7
			10000 ppm H_2S			
558	0.926	0.967	0.936	0.943	0.954	–1.2
673	0.995	0.981	0.983	0.986	0.965	2.1
923	0.987	0.979	0.988	0.985	0.988	-0.3
1173	0.991	0.983	0.991	0.988	0.992	–0.4

[a] Average uncertainties on XRD, microprobe, and combustion data are ± 0.9–2.0%, 1.5% and 0.4% respectively.

[b] Δ=100 (Observed–Predicted)/Observed.

n.a.: not analyzed.

S ratios. As discussed in Section 4 below, the sulfide layers crack when they cannot plastically deform into the void space at the metal/sulfide interface. The electron microprobe traverses of many samples show decreases in the Fe/S ratios from the metal/sulfide to sulfide/gas boundaries (*e.g.*, see Fig. 2 of LAURETTA *et al.* (1996b) in this volume). This gradient is present in samples that have either one or two sulfide layers and there is no discontinuity across the boundary between the two layers. Such profiles are expected from WAGNER's (1951) model for diffusion controlled reactions forming compact scale layers.

4. Microstructure and Morphology of Sulfide Layers

Experiments were done for different durations along several isotherms in all H_2S-H_2 gas mixtures to obtain information about the sulfide layer morphology produced from the reactions between H_2S gas and iron metal. This section describes the various sulfide layer morphologies observed.

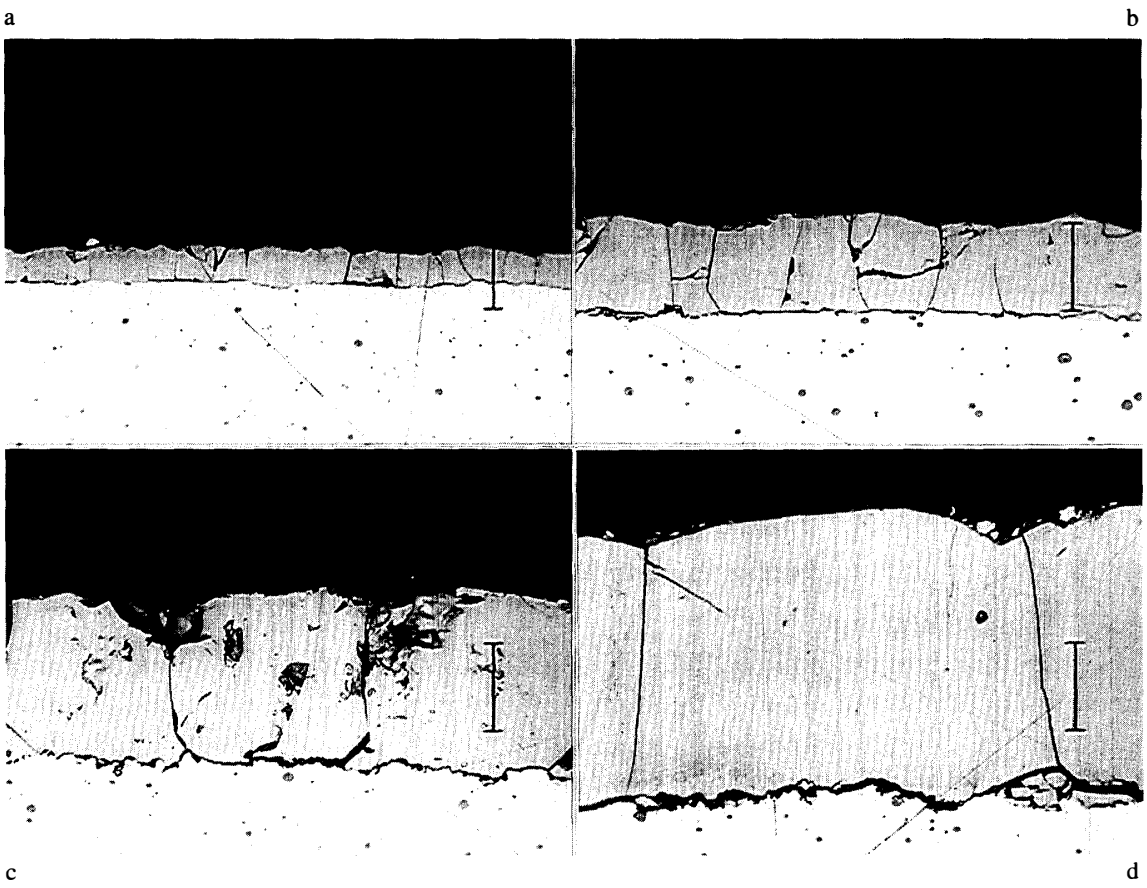

Figs. 2a–d. Reflected light optical photomicrographs illustrating the variation of sulfide layer thickness and microstructure with time for four samples isothermally heated at 923 K in an H_2S-H_2 gas mixture nominally containing 1000 ppmv H_2S. (a) 5 hours, (b) 12 hours, (c) 24 hours, (d) 48 hours. In each photograph the remaining metal lies along the bottom and the sulfide layer(s) lie above it. The black material at the top of each figure is epoxy. The scale bar is 32 μm in each photograph.

The initial sulfide layer consists of large compact crystals that are uniformly oriented along a specific crystallographic plane (*e.g.* (300) for samples formed in ~50 ppm H_2S at 558 and 614 K). This crystal orientation changes with formation conditions but this variation is not well characterized and the mechanism causing the change is still an open question (YOUNG, 1980). Figure 2 shows the variation of the sulfide layer thickness and microstructure with time for a sample reacted at 923 K in an H_2S-H_2 gas mixture nominally containing 1000 ppmv H_2S. The sulfide layers shown in Figs. 2a–2c show that up to the point where 20% of the metal has reacted, only one layer of sulfide crystals is present. However, as shown in Fig. 2d, a thin inner sulfide layer then begins to form. This inner layer consists of small, randomly oriented sulfide crystals separated by a large amount of void space. The thickness of the inner layer varies dramatically with the formation conditions. In some cases it is completely absent, while in other cases the inner layer can be as thick or thicker than the outer sulfide layer. A more detailed description of the observed variations in the thickness of the inner sulfide layer is given in LAURETTA *et al.* (1996a).

The formation of this two layer structure is a direct result of the reaction mechanism. Initially, H_2S reacts with the iron metal at the metal/gas interface. Once the metal is covered by sulfide, the layer grows by reaction of Fe^{2+} ions, that diffuse to the solid/gas interface, with sulfur (in the form of adsorbed H_2S or another adsorbed species such as HS or S). The outward diffusion of iron causes the metal surface to retreat back from the metal/sulfide interface. In order to fill the resulting gap, the sulfide layer must deform plastically into the newly created void space. Eventually, the limit of sulfide deformation is reached and vertical cracks form that extend from the outer edge of the sulfide layer down to the metal. These cracks allow gas to penetrate directly to the metal surface and form a new sulfide layer there. By this time, the metal surface has been roughened by the earlier formation of sulfide and the sulfide crystals in the new inner layer grow in random orientations. Eventually, the gap between the metal and sulfide is filled by the growth of the second layer and the growth, by outward diffusion of Fe^{2+} ions, of the outer layer resumes.

5. Kinetics and Mechanism of FeS Formation

5.1. Linear kinetics

The rate of formation of the sulfide layer is intimately connected to its growth mechanism. During the initial stages of the reaction, FeS formation is limited by the supply of sulfur at the metal-gas interface. This can be the result of several different rate-limiting mechanisms. The rate at which gas molecules collide with the metal surface, and the fraction of these collisions which possess the necessary activation energy to initiate a chemical reaction, may be the limiting factors. This is the case when the H_2S partial pressure is extremely low, and is the basis of the SCT model developed by FEGLEY (1988). At higher H_2S partial pressures, however, the rate of supply of gas molecules is no longer rate-limiting. Instead, the rate at which the H_2S molecules dissociate on the metal (or sulfide) surface is the rate-limiting step. The adsorption of H_2S and its subsequent dissociation proceeds by a series of elementary chemical reactions such as the following sequence (WORRELL and TURKDOGAN, 1968; WORRELL, 1971):

$$H_2S(gas) + \square \rightarrow H_2S(adsorbed), \quad (2)$$

$$H_2S(adsorbed) \rightarrow HS(adsorbed) + H(adsorbed), \quad (3)$$

$$HS(adsorbed) \rightarrow H(adsorbed) + S(adsorbed), \quad (4)$$

$$S(adsorbed) \rightarrow S + \square, \quad (5)$$

$$2H(adsorbed) \rightarrow H_2(gas), \quad (6)$$

where the $\square$ represents a vacant adsorption site on the metal (or sulfide) surface. WORRELL and TURKDOGAN (1968) found that reaction (3) is the rate-limiting step for FeS formation in H_2S-H_2 gas mixtures containing $\geq 1\%$ H_2S. In contrast, we find that step (2) is rate-limiting in 50–1000 ppmv H_2S gas mixtures with H_2 (*e.g.*, LAURETTA *et al.*, 1996a).

We determined the apparent linear rate constants for FeS formation from the weight gain and the fractional thickness change of the Fe foils. The two methods show excellent agreement and the derived rate constants are listed in Table 2. These rate constants are measurements of the net FeS formation rate for reaction (1) and are given by:

$$d(\Delta w/A)/dt = d(FeS)/dt = R_f - R_r = k_l, \quad (7)$$

where Δw is the measured weight gain, A is the geometric area of the Fe foil, t is time, R_i is the rate of the forward or reverse reaction and k_l is the apparent linear rate constant. As described by LAURETTA *et al.* (1996a) we also calculated the forward and reverse rate constants for reaction (1) by making use of the fact that FeS formation in H_2S-H_2 gas mixtures is an opposing first order reaction (WORRELL and TURKDOGAN, 1968; WORRELL, 1971). In the case of an opposing first order reaction (BENSON, 1960), eq. (7) can be rewritten as:

$$d(FeS)/dt = R_f - R_r = k_f P_{H_2S} - k_r P_{H_2}, \quad (8)$$

where k_i are the forward and reverse rate constants for FeS formation (with units such as cm hour^{-1}atm^{-1}) and P_i is the partial pressure of gas i. At the Fe-FeS phase boundary the net reaction rate is zero ($d(FeS)/dt=0$) and therefore $R_f=R_r$. For rate measurements in gas mixtures with H_2S/H_2 ratios much greater than the equilibrium ratio at the Fe-FeS boundary, eq. (8) reduces to:

$$d(FeS)/dt \sim k_f P_{H_2S}, \quad (9)$$

and k_f is directly determined. Our kinetic data in the nominal 100 and 1000 ppmv H_2S gas mixtures at several temperatures met this condition and we derived:

$$k_f = 5.6(\pm 1.3)\exp[-27950(\pm 7280)/RT], \quad (10)$$

where the activation energy is ~27950 J mole^{-1}. The reverse rate constant k_r was then calculated from the equilibrium constant (K_{eq}) for reaction (1) and the forward rate constant k_f as $k_r=(k_f/K_{eq})$:

$$k_r=10.3(\pm1.0)\exp[-92610(\pm350)/RT]. \quad (11)$$

TACHIBANA *et al.* (1995) studied troilite evaporation in H_2(g), for which eq. (11) should be valid, but do not give any rate constants to which we can compare our results.

Experiments done in gas mixtures containing 50 ppmv H_2S show a drastic increase in reaction rate at temperatures of 613 K and lower. This may be due to a change in the growth orientation of the sulfide crystals (see Table 2) or to vacancy ordering in the sulfide at low temperatures (BARKER and PARKS, 1986). Therefore, the reaction rates measured at temperatures less than 613 K in 50 ppmv H_2S are a factor of two higher than predicted by eqs. (10–11). The preliminary rate data obtained in 25 ppmv H_2S are presented in Table 2. However, each value was obtained from a single experimental sample and the errors are uncertain. As a result these data were not used in the calculation of k_f and k_r in eqs. (10) and (11).

Table 2. Apparent linear rate constants.

Temperature (K)	Apparent rate constant k (cm/hour)[d]	Temperature (K)	Apparent rate constant k (cm/hour)[d]
25 ppm H_2S		850 ppm H_2S	
558[a]	$(3.3)10^{-8}$	673	$(3.14\pm0.23)10^{-5}$
613[a]	$(5.0)10^{-8}$	778	$(6.85\pm2.48)10^{-5}$
643[a]	$(5.4)10^{-8}$	848	$(1.26\pm1.23)10^{-4}$
		923	$(1.05\pm0.54)10^{-4}$
50 ppm H_2S		10000 ppm H_2S	
558[b]	$(1.50\pm0.49)10^{-6}$	558	$(1.87\pm0.51)10^{-5}$
613[b]	$(2.66\pm0.50)10^{-6}$	673	$(2.35\pm1.94)10^{-5}$
643[c]	$(1.84\pm0.80)10^{-7}$		
673[c]	$(5.64\pm5.33)10^{-7}$		
100 ppm H_2S			
558	$(3.88\pm2.50)10^{-7}$		
658	$(1.59\pm0.14)10^{-6}$		
723	$(4.62\pm3.45)10^{-6}$		

[a] Only one data point. [b] Growth along *a*-axis.
[c] Growth along *c*-axis. [d] Errors are ±1 sigma.

5.2. *Parabolic kinetics*

During the later stages of FeS formation the behavior of the growth kinetics changes. This change takes place when the sulfide layer reaches a critical thickness and Fe^{2+} diffusion through the sulfide layer becomes slower than the rate of chemical reactions at the gas-solid boundary. Once diffusion is rate-limiting, FeS growth follows parabolic kinetics and the rate law becomes:

$$(\Delta w/A)^2=k_p t, \tag{12}$$

where k_p is the parabolic rate constant with units of $g^2\ cm^{-4}\ hour^{-1}$. We determined the critical sulfide layer thickness for transition from linear to parabolic kinetics at five different temperatures (558, 673, 773, 848, and 923 K) and also calculated the parabolic rate constants from the measured weight gains of the samples. Because of the exponential dependence of reaction rates and diffusion coefficients with temperature the critical layer thickness (t_{cr}) for the linear → parabolic transition is given as (LAURETTA *et al.*, 1996a):

$$t_{cr}=1033(\pm360)\exp[-2580(\pm295)/T]\mu m. \tag{13}$$

The kinetic data for samples formed in 1000 ppmv H_2S are shown in Fig. 3. The data are plotted as FeS layer thickness *vs.* time to illustrate the thickness at which the transition from parabolic to linear kinetic behavior occurs as a function of time at a given temperature. Figure 3 shows that the critical thickness varies from ~15±10 μm at 673 K to 64±15 μm at 923 K.

The parabolic rate constants are listed in Table 3. As Table 3 shows, we did not observe parabolic kinetics at all gas compositions and temperatures studied. This is because the sulfide layers formed at low temperatures in the lower concentration H_2S gas mixtures never reached the critical thicknesses where the transition to parabolic kinetics occurs. Presumably this would happen if the samples were reacted for much longer times, but these experiments are impractical for the lowest temperature runs in gas mixtures with very low H_2S concentrations.

Earlier in Section 3 we discussed a mechanism for the formation of bifurcated sulfide layers. This two layer structure probably explains why the rate constants at some temperatures and compositions have larger uncertainties than others. The general trend is that thicker outer layers form when growth of the sulfide is rapid, as is the case in the

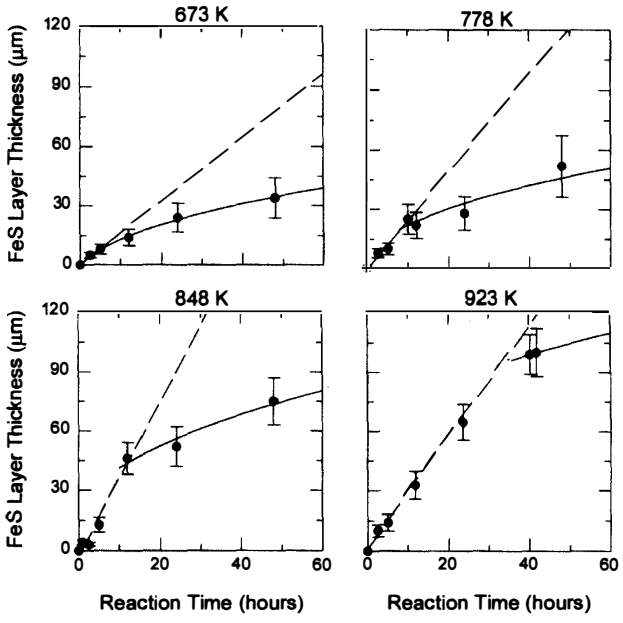

Fig. 3. Plots of FeS layer thickness versus time along four isotherms (673, 778, 848, and 923 K) for samples formed in ~1000 ppmv H_2S. The dashed lines show linear growth of the FeS layers with time. The solid lines show parabolic (i.e., diffusion controlled) growth of the FeS layers with time. The intersection of the two lines is the critical thickness at which FeS growth changes from linear to parabolic kinetics. The critical thicknesses vary from 15±12 μm at 673 K to 64±15 μm at 923 K.

Table 3. Parabolic rate constants.

Temperature (K)	Apparent rate constant k (cm^2/hour)	Temperature (K)	Apparent rate constant k (cm^2/hour)
850 ppm H_2S		10000 ppm H_2S	
673	$(9.83\pm9.83)10^{-8}$	558	$(4.58\pm0.43)10^{-8}$
778	$(1.29\pm0.79)10^{-7}$	923	$(9.31\pm3.61)10^{-6}$
848	$(5.34\pm3.30)10^{-7}$	1173[a]	$(5.77)10^{-5}$
923	$(4.94\pm0.37)10^{-7}$		
Activation energy: 38±13 kJ/mole		Activation energy: 63±1 kJ/mole	

[a]Only one point.

higher temperature runs in gas mixtures with larger H_2S concentrations. It may be that higher temperatures allow the sulfide layer to deform more easily, thus preventing catastrophic fracturing of the outer layer. The final morphology of the sulfide layer and the kinetic behavior are affected by the environment in which the sulfide formed, and a sulfide layer divided into two parts does not always form on the samples.

6. Applications to Troilite Formation in the Solar Nebula

6.1. Updated condensation calculations

We recalculated the troilite formation temperature and sulfur condensation in the solar nebula because of the recent publication of improved thermodynamic data for troilite and pyrrhotites (CEMIC and KLEPPA, 1988; GRØNVOLD and STØLEN, 1992; GRØNVOLD *et al.*, 1991) and because DREIBUS *et al.* (1995) recently revised the solar system abundance for sulfur. Troilite formation via reaction (1) occurs at 710 K from a metal alloy with the solar Fe/Ni ratio and at 713 K from pure iron metal. The 50% condensation temperature is 674 K, and sulfur is completely condensed into troilite by ~400 K. Hydrogen sulfide gas is the dominant sulfur gas over this temperature range, except at extremely low pressures (10^{-11} bars and below), that are implausible for the chondrite formation region in the solar nebula. Molecular S_2 becomes increasingly important at these very low pressures.

The sulfur condensation curve is illustrated in Fig. 4, which also shows the CI chondrite normalized S/Si ratios in the major chondrite groups. The S/Si ratios are tabulated in Table 4 which also gives the data sources used in the calculations. The well known variations in the sulfur content of chondritic material could be due to a number of factors such as the incomplete condensation of sulfur into grains in the solar nebula, the later loss of sulfur from these grains during subsequent heating in the solar nebula, or sulfur loss from chondrite parent bodies. Below we use our kinetic data to briefly discuss some of these alternative scenarios.

6.2. Rate of troilite formation in the solar nebula

Our kinetic data constrain the rate of iron sulfide formation in the solar nebula as a function of temperature, pressure, H_2S/H_2 ratio, and iron grain size. In Fig. 5 we plot the thickness of FeS layers formed on spherical Fe grains as a function of the extent of reaction of Fe to FeS. In the case of a 10 μm radius Fe grain, complete conversion to FeS

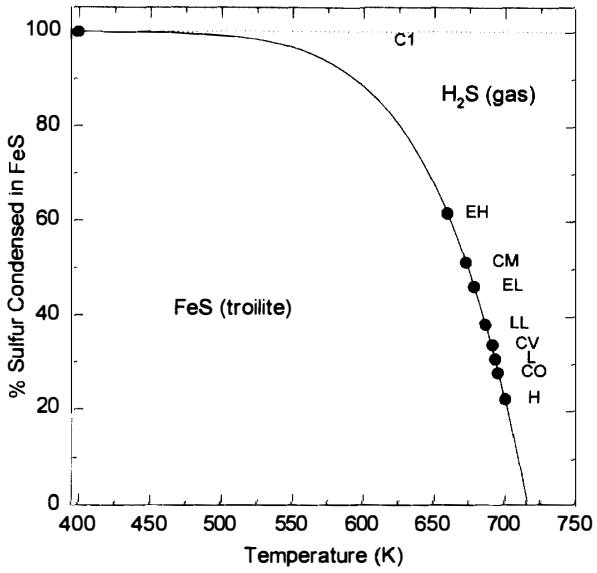

Fig. 4. The percentage of sulfur originally present as H_2S gas condensed into troilite as a function of temperature in the solar nebula. The sulfur condensation curve is pressure independent down to 10^{-11} bars total pressure. The black dots show the CI normalized S/Si ratios in the major chondrite groups. This ratio equals unity for 100% condensation of sulfur into troilite.

Table 4. S/Si ratios in chondrites.

Group	Ref.	S (wt%)	Si (wt%)	S/Si	$(S/Si)/(S/Si)_{CI}$
CI	a	5.41	10.5	0.515	=1.000
CM	a	3.21	12.9	0.249	0.483
CO	a	2.28	15.9	0.143	0.278
CV	a	2.25	15.6	0.144	0.280
H	b	2.0	16.9	0.118	0.211
L	b	2.2	18.5	0.119	0.212
LL	b	2.3	18.9	0.122	0.217
EH	b	5.8	16.7	0.347	0.618
EL	b	3.3	18.6	0.177	0.316

a: DREIBUS *et al.* (1995), b: WASSON and KALLEMEYN (1988).

yields 15.2 μm radius sulfide grain, while 50% conversion to FeS yields a metal-sulfide grain with a 7.94 μm radius metal core covered by a 5.17 μm thick FeS layer. The FeS layer thickness is independent of the rate at which the sulfide forms.

Overlain on the plot in Fig. 5 is the range of critical thickness values, determined from our experimental data, for the transition from linear to parabolic kinetic behavior. The extent of reaction at which the kinetic behavior changes from linear to parabolic is determined by the intersection of the FeS layer thickness curves with the observed range in the critical thickness values. Thus, FeS formation on small iron grains less than 10 μm in radius will always follow linear kinetics because, after complete conversion to FeS, the grains are smaller than the critical FeS thickness at which diffusion becomes the rate limiting step. Conversely, FeS formation on larger iron grains greater than 1000 μm radius will follow parabolic kinetics after only ~3% reaction because the FeS layers formed exceed the critical thickness after this small extent of reaction.

KERRIDGE (1993) used measurements of metal and silicate grain sizes in chondrites and interplanetary dust particles to infer grain sizes of metal and silicate in the solar nebula. The largest metal grains observed in type 3 and 4 chondrites are >400 μm in size

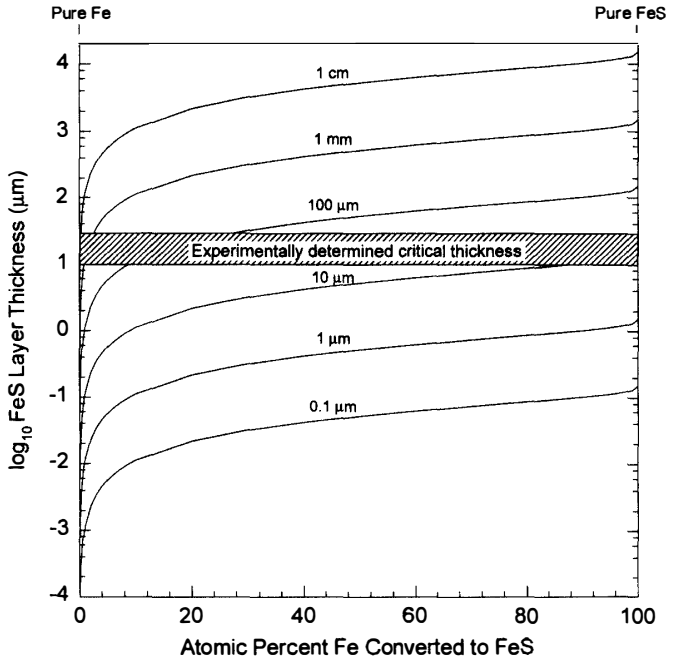

Fig. 5. The calculated FeS layer thicknesses on spherical iron grains of different sizes as a function of the extent of reaction is compared to the critical sulfide layer thickness at which a transition from linear to parabolic kinetics occurs. Iron sulfide formation from small metal grains, with radii of 10 μm and below always follows linear kinetics. Iron sulfide formation from larger metal grains initially follows linear kinetics until the critical thickness is reached, and then diffusion becomes rate limiting and parabolic kinetics is followed. The sulfidation of the largest metal grains, ~1000 μm in radius, begins to follow parabolic kinetics after only ~ 3% of the metal has been converted to FeS.

while the smallest grains in the matrix of unequilibrated ordinary chondrites are ~0.05 μm. Our experimental values for the critical thickness at which diffusion of Fe^{2+} becomes the rate limiting step imply that sulfurization of Fe grains smaller than 10 μm in radius will always proceed via linear kinetics. Using our experimentally determined linear rate constants (eqs. (10) and (11)) we calculate that a 10 μm grain will be completely converted to iron sulfide in ~200 years at 700 K and 10^{-3} atm. Similarly, sulfurization of an Fe grain with a radius of 1000 μm will follow parabolic kinetics after a very small extent of reaction. Using our experimentally determined parabolic rate constants (Table 3) we calculate that a grain of this size will be completely converted to FeS in ~500 years at 700 K in a gas of solar composition. Furthermore, if collisions with other grains lead to cracking and/or removal of the sulfide layer, the freshly exposed metal will then react with the H_2S gas via linear kinetics. Thus, the parabolic time constants (*e.g.*, 500 years for a 1000 μm grain) are best regarded as upper limits to the actual time required for FeS formation.

The linear rate constants measured in our experiments at ambient atmospheric pressure imply that the rate controlling mechanism at low H_2S mixing ratios (<1000 ppmv) is H_2S adsorption on the metal or sulfide surface. However, at the low pressures expected

for the solar nebula, the supply of H_2S molecules at the surface of the grain may limit the reaction rate. This is the mechanism modeled by FEGLEY's (1988) SCT model and we used a modified version of this model to provide a second estimate for times required to convert Fe to FeS in the solar nebula. Our experimentally determined value of ~28 kJ/mole for the activation energy of iron sulfide formation was used in the calculations. In addition, we considered the depletion of H_2S due to consumption during FeS formation. We modeled FeS formation in this manner for two extreme cases of spherical iron grains with radii of 0.1 μm (Fig. 6a) and 1000 μm (Fig. 6b). At each temperature considered the P_{H_2S}/P_{H_2} ratio starts at the solar value and decreases to the equilibrium value at the Fe-

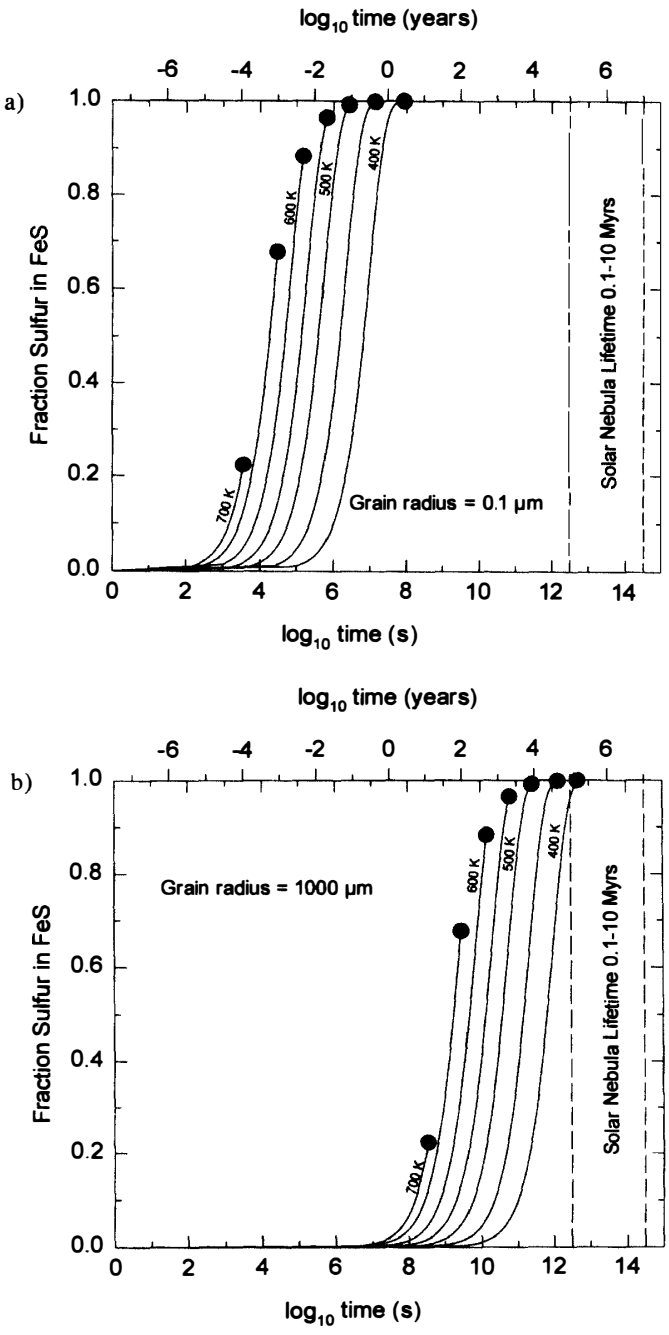

Figs. 6a, b. The amount of time required for different fractions of sulfur to condense into troilite in the solar nebula is plotted for two extreme cases of (a) 0.1 μm radius iron grains and (b) 1000 μm radius iron grains at different temperatures. Except perhaps for sulfidation of the largest grains at 400 K, sulfur condensation proceeds to the extent allowed by chemical equilibrium within the 0.1–10 million year lifetime of the solar nebula (indicated by the vertical dashed lines).

FeS phase boundary where FeS formation stops. The point at which this occurs is represented as a black dot on the isothermal curves in Figs. 6a and 6b. The black dots for each isotherm in Figs. 6a and 6b correspond to the percent sulfur condensed in FeS that is plotted in Fig. 4.

Thus at 700 K, Fig. 4 shows that FeS formation proceeds until ~22% of the H_2S has condensed as FeS and ~78% remains as H_2S gas. Figure 6a shows that FeS formation (consuming 22% of all available sulfur) takes ~3500 s (~1 hour) by reaction with 0.1 μm radius Fe grains and ~$10^{8.55}$ s (~11.33 years) by reaction with 1000 μm radius Fe grains.

Likewise, Fig. 4 shows that 100% of all H_2S condenses into FeS by 400 K. Figures 6a and 6b show that the reaction of H_2S with Fe grains at 400 K takes ~$10^{7.95}$ s (~2.8 years) for 0.1 μm radius Fe grains and ~$10^{12.69}$ s (~$10^{5.2}$ years) for 1000 μm radius Fe grains. With the exception of H_2S reacting with 1000 μm radius Fe grains at 400 K, all of these times are less than the 100000 year lower limit given by PODOSEK and CASSEN (1994) for the lifetime of the solar nebula.

Thus, it is unlikely that sulfur condensation into troilite was kinetically inhibited in the solar nebula. Our conclusions agree with the earlier result of FEGLEY (1988) who used the SCT model to argue that FeS formation was an extremely rapid process in the solar nebula. The rapid formation of troilite in turn implies that S/Si ratios lower than the CI value resulted from incomplete sulfur condensation due to removal of the solid grains from continued reaction with the nebular gas. While our data are not directly relevant to the question of sulfur loss by vaporization, PALME *et al.* (1988) have presented arguments against evaporative loss of volatile elements from chondritic material.

Acknowledgments

This work was supported by NASA Grant NAGW-3070. Dr. S. MATSUNAMI and an anonymous referee provided constructive reviews.

References

ANDERS, E. and Grevesse, N. (1989): Abundances of the elements: Meteoritic and solar. Geochim. Cosmochim. Acta, **53**, 197–214.

BARKER, W.W. and PARKS, T.C. (1986): The thermodynamic properties of pyrrhotite and pyrite: A re-evaluation. Geochim. Cosmochim. Acta, **50**, 2185–2194.

BENSON, S.W. (1960): The Foundations of Chemical Kinetics. New York, McGraw-Hill, 703 p.

CEMIC, L. and KLEPPA, O.J. (1988): High temperature calorimetry of sulfide systems III. Standard enthalpies of formation of phases in the systems Fe-Cu-S and Co-S. Phys. Chem. Miner., **16**, 172–179.

CHASE, M.W., Jr., DAVIES, C.A., DOWNEY, J.R., Jr., FRURIP, D.J., MCDONALD, R.A. and SYVERUD, A.N. (1985): JANAF Thermochemical Tables, 3rd ed. Am. Chem. Soc. and Am. Inst. Phys., 1856 p. (J. Phys. Chem. Ref. Data, **14**, supplement No. 1).

DREIBUS, G., PALME, H., SPETTEL, B., ZIPFEL, J. and WÄNKE, H. (1995): Sulfur and selenium in chondritic meteorites. Meteoritics, **30**, 439–445.

FEGLEY, B., Jr. (1988): Cosmochemical trends of volatile elements in the solar system. Workshop on The Origins of Solar Systems, ed. by J. A. NUTH and P. SYLVESTER. Houston, Lunar Planet. Inst., 51–60 (LPI Technical Report No. 88-04).

FEGLEY, B., Jr. (1993): Chemistry of the solar nebula. The Chemistry of Life's Origins, ed. by M. GREENBERG *et al.* Dordrecht, Kluwer, 75–147 (NATO Advance Science Institute Series C, Vol. 416).

FEGLEY, B., Jr. and PRINN, R.G. (1989): Solar nebula chemistry: Implications for volatiles in the solar system. The Formation and Evolution of Planetary Systems, ed. H. WEAVER and L. DANLY. Cambridge, Cambridge Univ. Press, 171–211.

GRØNVOLD, F. and STØLEN, S. (1992): Thermodynamics of iron sulfides II. Heat capacity and thermodynamic properties of FeS and of $Fe_{0.875}S$ at temperatures from 298.15 K to 1000 K, of $Fe_{0.98}S$ from 298.15 K to 800 K, and of $Fe_{0.89}S$ from 298.15 K to about 650 K. Thermodynamics of formation. J. Chem. Thermodyn., **24**, 913–936.

GRØNVOLD, F., STØLEN, S., LABBAN, A.K. and WESTRUM, E.F., Jr. (1991): Thermodynamics of iron sulfides I. Heat capacity and thermodynamic properties of Fe_9S_{10} at temperatures from 5 K to 740 K. J. Chem. Thermodyn., **23**, 261–272.

KERRIDGE, J.F. (1993): What can meteorites tell us about nebular conditions and processes during planetesimal accretion? Icarus, **106**, 135–150.

LAURETTA, D.S. and FEGLEY, B., Jr. (1994a): An experimental study of iron sulfide formation kinetics in H_2-H_2S gas mixtures and application to iron sulfide condensation in the solar nebula. Lunar and Planetary Science XXV. Houston, Lunar Planet Inst., 773–774.

LAURETTA, D.S. and FEGLEY, B., Jr. (1994b): Kinetics and grain growth mechanism for troilite formation on iron metal in H_2-H_2S gas mixtures. Papers presented to the 19th Symposium on Antarctic Meteorites, 30 May–1 June 1994. Tokyo, Natl. Inst. Polar Res., 62–65.

LAURETTA, D.S. and FEGLEY, B., Jr. (1994c): Troilite formation kinetics and growth mechanism in the solar nebula. Meteoritics, **29**, 490.

LAURETTA, D.S., KREMSER, D.T. and FEGLEY, B., Jr. (1995a): Nickel fractionation during troilite formation in the solar nebula. Lunar and Planetary Science XXVI. Houston, Lunar Planet Inst., 831–832.

LAURETTA, D.S., KREMSER, D.T. and FEGLEY, B., Jr. (1995b): The origin of troilite and pyrrhotite in chondrites: II. Comparative studies of metal-sulfide assemblages. Antarctic Meteorites XX. Tokyo, Natl. Inst. Polar Res., 134–137.

LAURETTA, D.S., KREMSER, D.T. and FEGLEY, B., Jr. (1996a): The rate of iron sulfide formation in the solar nebula. Icarus (in press).

LAURETTA, D.S., KREMSER, D.T. and FEGLEY, B., Jr. (1996b): A comparative study of experimental and meteoritic metal-sulfide assemblages. Proc. NIPR Symp. Antarct. Meteorites, **9**, 97–110.

LEWIS, J.S. and PRINN, R.G. (1980): Kinetic inhibition of CO and N_2 reduction in the solar nebula. Astrophys. J., **238**, 357–364.

LIBOWITZ, G.G. (1972): Energetics of defect formation and interaction in non-stoichiometric pyrrhotite. Reactions of Solids, ed. by J.S. ANDERSON *et al.* London, Chapman and Hall, 107–115.

PALME, H., LARIMER, J.W. and LIPSCHUTZ, M.E. (1988): Moderately volatile elements. Meteorites and the Early Solar System, ed. by J. F. KERRIDGE and M. S. MATTHEWS. Tucson, University of Arizona Press, 436–461.

PODOSEK, F.A. and CASSEN, P. (1994): Theoretical, observational, and isotopic estimates of the lifetime of the solar nebula. Meteoritics, **29**, 6–25.

PRINN, R.G. and FEGLEY, M.B. (1981): Kinetic inhibition of CO and N_2 reduction in circumplanetary nebulae: Implications for satellite composition. Astrophys. J., **249**, 308–317.

PRINN, R.G. and FEGLEY, B., Jr. (1987): The atmospheres of Venus, Earth, and Mars: A critical comparison. Ann. Rev. Earth Planet. Sci., **15**, 171–212.

PRINN, R.G. and FEGLEY, B., Jr. (1989): Solar nebula chemistry: Origin of planetary, satellite, and cometary volatiles. Origin and Evolution of Planetary and Satellite Atmospheres, ed. by S.K. ATREYA *et al.* Tucson, Univ. Arizona Press, 78–136.

RAU, H. (1976): Energetics of defect formation and interaction in pyrrhotite $Fe_{1-x}S$ and its homogeneity range. J. Phys. Chem. Solids, **37**, 425–429.

TACHIBANA, S., TSUCHIYAMA, A. and KITAMURA, M. (1995): Incongruent evaporation experiments on troilite (stoichiometric FeS). Antarctic Meteorites XX. Tokyo, Natl. Inst. Polar Res., 235–238.

UREY, H.C. (1952): The Planets. Their Origin and Development. New Haven, Yale University Press.

UREY, H.C. (1953): Chemical evidence regarding the Earth's origin. Intl. Conf. Pure and Applied Chem. and Plenary Lectures XIII. Stockholm, Almquist and Wiksells, 188–217.

WAGNER, C. (1951): Diffusion and high temperature oxidation of metals. Atom Movements. Cleveland,

American Society for Metals, 153–173.

WASSON, J.T. and KALLEMEYN, G.W. (1988): Compositions of chondrites. Philos. Trans. R. Soc. London, **A325**, 535–544.

WORRELL, W.L. (1971): Dissociation of gaseous molecules on solids at high temperature. Advances in High Temperature Chemistry Vol. 4, ed. by L. EYRING. New York, Academic Press, 71–105.

WORRELL, W.L. and TURKDOGAN, E.T. (1968): Iron sulfur system part II. Rate of reaction of hydrogen sulfide with ferrous sulfide. Trans. AIME, **242**, 1673–1678.

YOUNG, D.J. (1980): The sulfidation of iron and its alloys. Rev. High Temp. Mater., **4**, 299–346.

(Received September 18, 1995; Revised manuscript accepted November 6, 1995)